Journal of Applied Remote Sensing

RemoteSensing.SPIEDigitalLibrary.org

General three-layer scattering model for forest parameter estimation using single-baseline polarimetric interferometry synthetic aperture radar data

Nghia Pham Minh
Bin Zou
Yan Zhang
Vannhu Le

SPIE.

General three-layer scattering model for forest parameter estimation using single-baseline polarimetric interferometry synthetic aperture radar data

Nghia Pham Minh,[a,*] Bin Zou,[b] Yan Zhang,[b] and Vannhu Le[c]

[a]Le Qui Don Technical University, Faculty of Radio-Electronics, Department of Circuits and Signal Processing, 236 Hoang Quoc Viet Street, Hanoi, Vietnam

[b]Harbin Institute of Technology, Department of Information Engineering, Harbin 15001, China

[c]Harbin Institute of Technology, Research Center for Space Optics Engineering, Harbin 15001, China

Abstract. The random volume over ground (RVoG) model has been extensively applied to polarimetric interferometry SAR (PolInSAR) data for the retrieval of forest geophysical parameters. The complex interferometric coherence of the RVoG model was originally derived in a simplified way by neglecting one of the two possible contributions of the ground response: direct return from the ground or double-bounce interaction with the stems or trunks. In many cases, their influence depends on both the system and scene parameters, and none of them should be ignored *a priori*. Therefore, a more general model accounting for the simultaneous retrieval of the both ground contributions should be considered. Based on the characteristics of the scattering progress in the forest area, a general three-layer scattering model (GTLSM) is proposed to extract forest parameters using L-band single-baseline PolInSAR data. The proposed model assumes the vertical structural forest composed of three layers: canopy, tree-trunk, and ground layer, which account for the simultaneous effects of three scattering components on complex coherence. The GTLSM performance is evaluated with simulated data from PolSARProSim software and spaceborne data acquired by the SIR-C/X-SAR system. Experimental results indicate that forest parameters could be effectively extracted by the proposed GTLSM. [DOI: 10.1117/1.JRS.9.096043]

Keywords: polarimetric interferometry synthetic aperture radar; adaptive decomposition; forest height estimation; coherence matrix; scattering model.

Paper 14608 received Oct. 13, 2014; accepted for publication Apr. 24, 2015; published online May 28, 2015.

1 Introduction

Forest distributed over the continental surface constitutes an important dynamic carbon storage, the stocks and fluxes of which must be quantified for a better understanding of the terrestrial carbon cycle.[1,2] Forest height is important information for many forest management activities and is a critical parameter in modeling of ecosystem procedures. Polarimetric interferometric synthetic aperture radar (PolInSAR) systems have shown a great potential for forest height retrieval as it is sensitive to the vertical structure and physical characteristics of the scattering media. Recently, great numbers of approaches for forest height estimation using single-baseline PolInSAR data have been proposed, such as three-stage inversion process,[3] ESPRIT,[4–6] forest parameters inversion methods,[7–9] and model-based decomposition techniques.[10] Among them, the three-stage inversion process proposed by Cloude and Papathanassiou is quite simple and most widely used. This method divides the inversion process into three steps, which involves taking observation of the complex coherence values at a number of difference polarization channels and then minimizing the difference between the model predictions and observation in a least-squares sense. Accurate forest height estimation of the three-stage inversion process

*Address all correspondence to: Nghia Pham Minh, E-mail: nghiapmhvktqs@yahoo.com

1931-3195/2015/$25.00

depends greatly on the accurate estimation of model prediction. Furthermore, the estimation of volume decorrelation by using the three-stage inversion process is not much reliable, and there is an ambiguity zone of volume decorrelation. Besides, the forest height estimation using ESPRIT, proposed by Yamada,[4–6] can detect the local scattering centers corresponding to the canopy top and ground in the forest area, but the accuracy of this method becomes inappropriate by the closer two phase centers. These methods tend to underestimate the forest height due to attenuation of electromagnetic in the ground medium and the accuracy of these methods become inappropriate for dense forest region due to overestimate of the volume scattering contribution. In 2003, Cloude and Papathanassiou introduced the two-layer random volume over ground (RVoG) model for vegetated areas.[3] In this model, they assumed that the canopy extends from the crown to the ground. However, a natural forest has significant species and age-related variations in vertical structure. In order to match the scattering process in the natural forest, they added an extra phase parameter to the two-layer RVoG model, essentially making it a three-layer RVoG model. The essential modification is to move the canopy phase away from the ground phase and this introduces a new phase parameter. This phase is defined as a boundary between the canopy and trunk layer. Nevertheless, the boundary between trunk and canopy layer is not explicitly defined for the natural structure of forest. Additionally, the complex interferometric coherence of these models is derived under the assumption that the ground response is dominated by one of two possible contributions: direct return from the ground surface or double-bounce interaction between the ground and trunk or stems. However, in many cases, particularly forest scattering at the L-band, the effect of the both the ground scattering and double-bounce scattering component is present. For instance, at 40 to 45 deg of incidence angle and when the ground is not especially rough, the direct ground response is negligible when compared to the double-bounce scattering component.[11] However, this situation changes when steeper incidence angles are used, since the direct ground backscatter also becomes noticeable. Therefore, a more general model for the considering the simultaneous effect of the both types of ground contribution is required.

For these reasons, a general three-layer scattering model (GTLSM) is proposed, which intend to express for describing the complex interferometric coherence of an RVoG when the ground contribution is a combination of both the double-bounce mechanism and the direct return from the ground. In the GTLSM, the vertical structure of forest comprises three layers such as canopy, tree-trunk, and ground layer, which account for the simultaneous effect of three scattering mechanisms in the forest area. The GTLSM enables the retrieval of not only the forest height but also the magnitude associated with each mechanism: single-bounce, double-bounce, and volume scattering mechanism.

The organization of the paper is as follows. In Sec. 2, the general three-layer forest scattering model is presented. Forest height extraction based on GTLSM is introduced in Sec. 3. The experimental results of estimating forest parameters are described in Sec. 4. Finally, several conclusions are given in Sec. 5.

2 General Three-Layer Scattering Model

2.1 *Complex Polarimetric Interferometric Coherence*

A monostatic, fully polarimetric interferometric SAR system is measured for each resolution cell in the scene from two slightly different look angles, two scattering matrices $[S_1]$ and $[S_2]$. In the case of backscattering in a reciprocal medium, the individual polarimetric data sets may be expressed by means of the Pauli target vector.[12]

$$\vec{k}_i = \frac{1}{\sqrt{2}}[S^i_{\mathrm{hh}} + S^i_{\mathrm{vv}} S^i_{\mathrm{hh}} - S^i_{\mathrm{vv}} 2S^i_{\mathrm{hv}}]^T, \tag{1}$$

where $(\bullet)^T$ represents the vector transposition, $S_{pq}(p, q = \{h, v\})$ are the complex scattering coefficients, and $i = 1, 2$ denote measurements at two ends of the baseline.

The basic radar observable in PolInSAR is a six-dimension complex matrix of a pixel in each resolution element in the scene, defined as shown in Eq. (2):

$$[T] = \langle \vec{k}.\vec{k}^{*T} \rangle = \begin{bmatrix} T_1 & \Omega \\ \Omega^{*T} & T_2 \end{bmatrix} \quad \text{with} \quad \vec{k} = \begin{bmatrix} \vec{k}_1 \\ \vec{k}_2 \end{bmatrix}, \tag{2}$$

where $\langle \bullet \rangle$ denotes the ensemble average in the data processing and $(\bullet)^*$ represents the complex conjugation. The matrices T_1 and T_2 are the conventional Hermitian polarimetric coherence matrices, which describe the polarimetric properties for each individual image separately. While Ω is a non-Hermitian complex matrix, which contains polarimetric and interferometric information.

In general, the complex polarimetric interferometric coherence as a function of the polarization of the two images is given by[13]

$$\tilde{\gamma}(\vec{\omega}) = \frac{\vec{\omega}_1^{*T} \Omega \vec{\omega}_2}{\sqrt{(\vec{\omega}_1^{*T} T_1 \vec{\omega}_1)(\vec{\omega}_2^{*T} T_2 \vec{\omega}_2)}} = \frac{\vec{\omega}^{*T} \Omega \vec{\omega}}{\vec{\omega}^{*T} T \vec{\omega}}, \tag{3}$$

where $\vec{\omega}_1 = \vec{\omega}_2 = \vec{\omega}$ is a three-component unitary complex vector defining the selection of each polarization stage and $T = (T_1 + T_2)/2$.

2.2 *General Three-Layer Scattering Model*

In the two-layer RVoG model, polarimetric coherence matrices and polarimetric interferometric coherence matrix related to the ground and volume scattering components are defined as[3]

$$T = I_1^V + e^{-\frac{2\sigma h_v}{\cos\theta}} I_1^G \quad \Omega = e^{j\phi_v} I_2^V + e^{j\phi_g} e^{-\frac{2\sigma h_v}{\cos\theta}} I_2^G, \tag{4}$$

where I_i^G $(i = 1, 2)$ are the scattering components of ground contribution, which is derived under the assumption that the ground response is dominated by one of two possible contributions: direct return from the ground or double-bonce interaction between ground and trunk. I_i^V $(i = 1, 2)$ denote the volume scattering from canopy layer. The angle θ denotes the incidence angle. The angles ϕ_g and ϕ_v are the phase centers of the ground and canopy layer, respectively.

As shown in Fig. 1, in the forest scattering at L-band, the backscattered waves can be considered as the direct scattering return from the ground (g), the double-bounce scattering between the ground and the tree trunks or branches (d), and the volume scattering from canopy (v). In Fig. 1, h_v is the height of forest, h_d is the height of tree trunk (not necessary equal to the height of bottom canopy layer), and z_c denotes the height of the bottom canopy layer. The black paths and the red paths represent the true wave paths and the effective wave paths for different component types, respectively. As can be seen, for the surface and volume component, the apparent heights correspond to the true scatterer heights, whereas for the double-bounce component, the apparent height is located at the ground level, due to the specular reflection at the ground. The proposed GTLSM can be generated by making the following assumptions about the three-layer scattering problem: (1) assume dual transmitter operation only. Both the direct surface and the double-bounce scattering contributions have structure functions given by a Dirac delta function, (2) assume an exponential structure function for direct volume return. It can be characterized by a mean wave extinction σ, which may nonetheless be a function of polarization, and (3) assume the layer is lossy enough and the surface rough enough that third- and higher-order interaction can be ignored. The polarimetric coherence matrix and polarimetric interferometric matrix in Eq. (4) then become

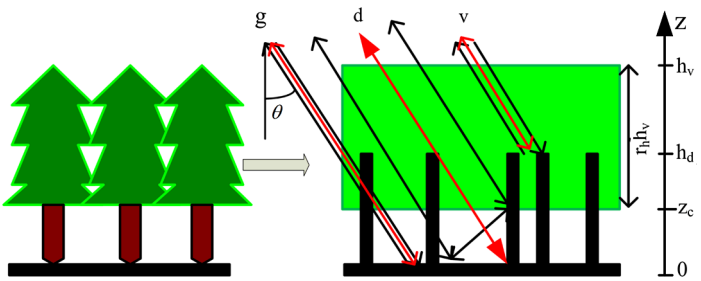

Fig. 1 Three-layer scattering model in forest area: ground, trunk, and canopy layer.

$$T = I_1^V + e^{-\frac{2\sigma h_v}{\cos\theta}} I_1^G + e^{-\frac{2\sigma h_v}{\cos\theta}} I_1^D$$
$$\Omega = e^{j\phi_v} I_2^V + e^{j\phi_g} e^{-\frac{2\sigma h_v}{\cos\theta}} I_2^G + e^{j\phi_d} e^{-\frac{2\sigma h_v}{\cos\theta}} I_2^D, \quad (5)$$

where I_i^D $(i = 1, 2)$ are the scattering components of double-bounce scattering. By assuming a random volume for canopy layer, the propagation factor for the direct surface and double-bounce interaction between the ground and tree-trunks is the same and function of a single-mean extinction coefficient σ, which are equal $e^{-(2\sigma h_v/\cos\theta)}$.

Comparing Eq. (5) with two-layer RVoG model, I_i^D is a new scattering component, which accounts for the effect of the double-bounce interaction between the ground and tree-trunks or branches into the forest scattering model. In the proposed GTLSM, the top boundary of trunk layer can be set at the first branching point, where the trunk divides into multiple large branches. Therefore, the top boundary of trunk layer can lie in the canopy layer, which shows that GTLSM is more appropriate for describing the scattering process in the natural forest area. The angles ϕ_g, ϕ_d and ϕ_v are the phase centers of the ground layer, tree-trunk layer, and canopy layer, respectively

$$I_1^V = e^{-\frac{2\sigma r_h h_v}{\cos\theta}} \int_0^{r_h h_v} e^{\frac{2\sigma z'}{\cos\theta}} T_v dz',$$
$$I_2^V = e^{-\frac{2\sigma r_h h_v}{\cos\theta}} e^{j(1-r_h)k_z h_v} \int_0^{r_h h_v} e^{\frac{2\sigma z'}{\cos\theta}} e^{jk_z z'} T_v dz',$$
$$I_1^G = \int_0^{h_v} \delta(z') e^{\frac{2\sigma z'}{\cos\theta}} T_g dz' = T_g; \quad I_2^G = T_g,$$
$$I_1^D = \int_0^{h_d} \delta(z') e^{\frac{2\sigma z'}{\cos\theta}} T_d dz' = T_d; \quad I_2^D = T_d, \quad (6)$$

where k_z, σ are the vertical wavenumber of interferometer and the mean wave extinction in the medium, respectively. T_g, T_d, and T_v are the coherence matrix for the single-bounce, double-bounce, and volume scattering component, respectively. As shown in Fig. 1, the forest is modeled by three layers, which consist of the canopy, tree-trunk, and ground layers. The canopy layer is characterized by particle scattering anisotropy, the degree of orientation randomness, total forest height h_v, and the canopy-fill-factor ratio $r_h \in [0,1]$, which can be expressed as

$$r_h = \frac{h_v - z_c}{h_v}. \quad (7)$$

As discussed in Ref. 14, the relative elevation of the basic crown is linked to the forest height by one of the Nezer forest-specific allometric equations. This means that the allometric relationships for branch and tree woody biomass follow a logarithmic law. Therefore, if mean forest height $\bar{h}_v$ is known, the coefficient r_h will be determined as follows:

$$r_h = \frac{2.7\ \ln(\bar{h}_v) - 0.1}{h_v}. \quad (8)$$

By combining Eqs. (3), (5), and (6), the complex interferometric coherence for GTLSM in a forest area can be derived as

$$\tilde{\gamma}^{\mathrm{GTLSM}}(\vec{\omega}) = \frac{\vec{\omega}^{*T}\Omega\vec{\omega}}{\vec{\omega}^{*T}T\vec{\omega}}$$
$$= \frac{e^{j\phi_v}\vec{\omega}^{*T}I_2^V\vec{\omega} + e^{j\phi_g}e^{-\frac{2\sigma h_v}{\cos\theta}}\vec{\omega}^{*T}I_2^G\vec{\omega} + e^{j\phi_d}e^{-\frac{2\sigma h_v}{\cos\theta}}\vec{\omega}^{*T}I_2^D\vec{\omega}}{\vec{\omega}^{*T}I_1^V\vec{\omega} + e^{-\frac{2\sigma h_v}{\cos\theta}}\vec{\omega}^{*T}I_1^G\vec{\omega} + e^{-\frac{2\sigma h_v}{\cos\theta}}\vec{\omega}^{*T}I_1^D\vec{\omega}}$$
$$= \frac{e^{j\phi_v}\frac{\vec{\omega}^{*T}I_2^V\vec{\omega}}{\vec{\omega}^{*T}I_1^V\vec{\omega}} + e^{j\phi_g}e^{-\frac{2\sigma h_v}{\cos\theta}}\frac{\vec{\omega}^{*T}I_2^G\vec{\omega}}{\vec{\omega}^{*T}I_1^V\vec{\omega}} + e^{j\phi_d}e^{-\frac{2\sigma h_v}{\cos\theta}}\frac{\vec{\omega}^{*T}I_2^D\vec{\omega}}{\vec{\omega}^{*T}I_1^V\vec{\omega}}}{1 + e^{-\frac{2\sigma h_v}{\cos\theta}}\frac{\vec{\omega}^{*T}I_1^G\vec{\omega}}{\vec{\omega}^{*T}I_1^V\vec{\omega}} + e^{-\frac{2\sigma h_v}{\cos\theta}}\frac{\vec{\omega}^{*T}I_1^D\vec{\omega}}{\vec{\omega}^{*T}I_1^V\vec{\omega}}}$$
$$= \frac{e^{j\phi_v}e^{j\phi_c}\tilde{\gamma}_v + e^{j\phi_g}m_1(\vec{\omega}) + e^{j\phi_d}m_2(\vec{\omega})}{1 + m_1(\vec{\omega}) + m_2(\vec{\omega})}, \quad (9)$$

where $m_1(\vec{\omega})$ and $m_2(\vec{\omega})$ denote the effective ground-to-volume amplitude ratio and double-bounce scattering-to-volume amplitude ratio, respectively, and are expressed as follows:

$$m_1(\vec{\omega}) = e^{-\frac{2\sigma h_v}{\cos\theta}} \frac{\vec{\omega}^{*T} T_g \vec{\omega}}{\vec{\omega}^{*T} I_1^V \vec{\omega}} \quad \text{and} \quad m_2(\vec{\omega}) = e^{-\frac{2\sigma h_v}{\cos\theta}} \frac{\vec{\omega}^{*T} T_d \vec{\omega}}{\vec{\omega}^{*T} I_1^V \vec{\omega}}. \tag{10}$$

From Eq. (9), we can obtain the complex coherence for the volume alone $\tilde{\gamma}_v$ and a new phase parameter ϕ_c as shown in Eq. (11). The complex coherence for the volume alone $\tilde{\gamma}_v$ is the function of the extinction coefficient for random volume and its thickness $r_h h_v$. The coefficient ϕ_c is the phase of bottom of the canopy layer in the GTLSM, which depends on the vertical wavenumber and thickness of the canopy layer

$$\begin{aligned}
\frac{\vec{\omega}^{*T} I_2^V \vec{\omega}}{\vec{\omega}^{*T} I_1^V \vec{\omega}} &= e^{jk_z h_v (1-r_h)} \frac{\int_0^{r_h h_v} e^{\frac{2\sigma z'}{\cos\theta}} e^{jk_z z'} T_v dz'}{\int_0^{r_h h_v} e^{\frac{2\sigma z'}{\cos\theta}} T_v dz'} = \tilde{\gamma}_v e^{j\phi_c} \\
\tilde{\gamma}_v &= \frac{I}{I_0} = \begin{cases} I = \int_0^{r_h h_v} e^{\frac{2\sigma z'}{\cos\theta}} e^{jk_z z'} T_v dz' \\ I_0 = \int_0^{r_h h_v} e^{\frac{2\sigma z'}{\cos\theta}} T_v dz' \end{cases} \\
\phi_c &= k_z h_v (1 - r_h).
\end{aligned} \tag{11}$$

Figure 2 shows the relationship between the complex polarimetric interferometric coherence and effective amplitude of the ratio of ground-to-volume and double-bounce scattering-to-volume. As outlined in Fig. 2, when $m_1(\vec{\omega})$ and $m_2(\vec{\omega})$ approach zero, the complex polarimetric interferometric coherence is nearly constant. The limit of the interferometric coherence can be deserved from Eq. (9):

$$\lim_{\substack{m_1(\vec{\omega}) \to 0 \\ m_2(\vec{\omega}) \to 0}} \tilde{\gamma}^{\text{GTLSM}} = e^{j\phi_v} e^{j\phi_c} \tilde{\gamma}_v. \tag{12}$$

Compared with the three-layer RVoG model in Ref. 3, it is clear that when the canopy layer may be extended from crown to the ground and the phase of the bottom of the tree-trunk layer can be located at ground level, $\phi_g = \phi_d = \phi_v = \phi_0$. Then, GTLSM becomes exactly the same as the three-layer RVoG,[3] as represented in Eq. (13), whereas when $m_1(\vec{\omega})$ or $m_2(\vec{\omega})$ are constant, the locus of the interferometric coherence represents a straight line inside the unit circle in the complex coherence plane.[3]

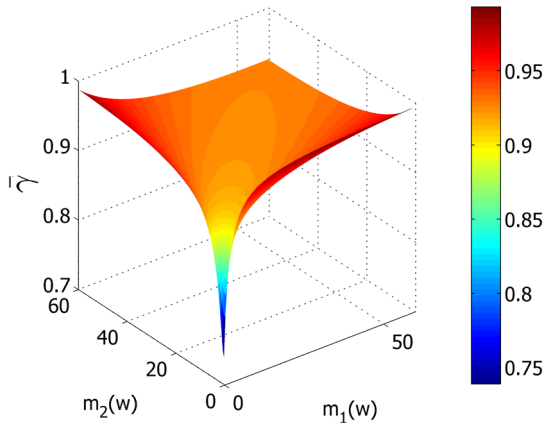

Fig. 2 Coherence amplitude variation against $m_1(\vec{\omega})$ and $m_2(\vec{\omega})$ in the scattering model.

$$\tilde{\gamma}^{\mathrm{GTLSM}} = e^{j\phi_0}\frac{e^{j\phi_c}\tilde{\gamma}_{\mathrm{v}} + m(\vec{\omega})}{1 + m(\vec{\omega})} \quad \text{with} \quad m(\vec{\omega}) = m_1(\vec{\omega}) + m(\vec{\omega}_2). \tag{13}$$

The proposed GTLSM divides the vertical structure of forest into three layers: canopy, tree-trunk, and ground layer, which account for the simultaneous effects of three scattering components in forest area: volume scattering, double-bounce ground trunk interaction, and direct ground scattering. Based on Eqs. (5) to (13), we show that the proposed GTLSM is more suitable and effective for analysis of scattering process in a natural forest. The inversion model for GTLSM can be formulated as follows:[12]

$$\begin{aligned} &\underline{p} = M^{-1}\underline{o} \\ &\underline{p} = \{\sigma, h_{\mathrm{v}}, h_{\mathrm{d}}, \phi_{\mathrm{g}}, m_1^k, m_2^k\} \quad k = 1,2,3 \\ &\underline{o} = \{\tilde{\gamma}_1, \tilde{\gamma}_2, \tilde{\gamma}_3\}, \end{aligned} \tag{14}$$

where the operator $[M]$ represents the scattering model, as given in Eqs. (9) to (11). The model relates to the three optimal complex coherences ($\tilde{\gamma}_j$, $j = 1,2,3$) obtained by polarimetric interferometric phase coherence optimization to 10 unknown parameters $\{\sigma, h_{\mathrm{v}}, h_{\mathrm{d}}, \phi_{\mathrm{g}}, m_1^k, m_2^k\}$ ($k = 1,2,3$) of the scattering process. This is a nonlinear parameter optimization problem. Therefore, to accurately extract forest parameters, the canopy phase and volume scattering coherence matrix are extracted by the adaptive model-based decomposition approach,[15] whereas the parameters of single- and double-bounce scattering contribution are estimated by the nonlinear least-squares optimization method.[16] Then the underlying ground topography phase can be estimated by using the cancellation of scattering mechanism method.[17,18]

3 Forest Height Estimation Based on GTLSM

3.1 *Canopy Phase Estimation from PolInSAR Data Using Adaptive Model-Based Decomposition*

For PolInSAR data, the polarimetric coherence matrices and polarimetric interferometric coherence matrix are decomposed into the three scattering mechanisms corresponding to single-bounce, double-bounce, and volume scattering

$$\begin{aligned} T &= f_{\mathrm{g}}T_{\mathrm{g}} + f_{\mathrm{d}}T_{\mathrm{d}} + f_{\mathrm{v}}T_{\mathrm{v}} \\ \Omega &= e^{j\phi_{\mathrm{g}}}f_{\mathrm{g}}T_{\mathrm{g}} + e^{j\phi_{\mathrm{d}}}f_{\mathrm{d}}T_{\mathrm{d}} + e^{j\phi_{\mathrm{v}}}f_{\mathrm{v}}T_{\mathrm{v}}, \end{aligned} \tag{15}$$

where f_{g}, f_{d}, and f_{v} represent the scattering power coefficient of single-bounce, double-bounce, and volume scattering, respectively.

The volume scattering is direct diffuse scattering from the canopy layer of the forest model. Theoretically, the scattering from the canopy layer of the forest can be characterized by a cloud of randomly oriented infinitely thin cylinders, and it is implemented with a uniform probability function for orientation angle.[19] However, for forest areas where vertical structure seems to be rather dominant, the scattering from tree-trunks and branches display a nonuniform angle distribution. Therefore, we assume that the volume scattering contribution with the n'th power cosine-square distribution of orientation with probability density function is as in Ref. 20. This function can be characterized by two parameters: the mean orientation of particles $\bar{\theta}$ and the degree of orientation randomness ν. The mean orientation of particles $\bar{\theta} \in [-\pi/2; \pi/2]$ and the degree of orientation randomness vary over a range between 0 and 0.91. In order to improve the general for volume scattering contribution, we add the particle scattering anisotropy into the volume scattering contribution introduced by Arri.[21] Therefore, T_{v} is a generalized volume scattering matrix, which depends on the mean orientation angle, degree of randomness, and the particle scattering anisotropy δ. Then, the volume scattering coherence matrix is given by

$$T_{\mathrm{v}}(\bar{\theta}, \nu) = T_a + p(\nu)T_b(2\bar{\theta}) + q(\nu)T_c(\bar{\theta}), \tag{16}$$

where the coefficients $p(\nu)$ and $q(\nu)$ are characteristics by sixth-order polynomials as in Ref. 20. The basic coherence matrices T_a, T_b, and T_c are expressed as

$$T_a = \frac{1}{4}\begin{bmatrix} 2 & 0 & 0 \\ 0 & |\delta|^2 & 0 \\ 0 & 0 & |\delta|^2 \end{bmatrix},$$
$$T_b = \frac{1}{4}\begin{bmatrix} 0 & 2\delta \cos 2\bar{\theta} & -2\delta \sin 2\bar{\theta} \\ 2\delta^* \cos 2\bar{\theta} & 0 & 0 \\ -2\delta^* \sin 2\bar{\theta} & 0 & 0 \end{bmatrix},$$
$$T_c = \frac{1}{4}\begin{bmatrix} 0 & 0 & 0 \\ 0 & |\delta|^2 \cos 4\bar{\theta} & -|\delta|^2 \sin 4\bar{\theta} \\ 0 & -|\delta|^2 \sin 4\bar{\theta} & -|\delta|^2 \cos 4\bar{\theta} \end{bmatrix}. \quad (17)$$

The particle scattering anisotropy magnitude $|\delta|$ is directly related to Cloude's α angle,[22] $|\delta| = \tan \alpha$, and $\arg(\delta) = \arg(\langle (S_{hh} + S_{vv}) S_{hv}^* \rangle)$.

Based on the assumption for volume scattering mechanism, we shall develop an adaptive model-based decomposition algorithm to estimate parameters of canopy layer. First, we use Eq. (16) to find the volume scattering coherence matrix. In particular, in forest areas, the backscattering of an electromagnetic wave depends on the shape, size, and orientation of the leaves, small branches and tree-trunks. Cross-polar response is generated by volume scatter.[23] Therefore, we employed a generalized volume scattering mechanism model in Eq. (18) as a reference volume scattering model.[24] The reference volume scattering model is derived under the assumption that the surface scattering and double-bounce scattering are as introduced by Freeman and Durden.[19] The model does not require any geophysical media symmetry assumption. Under the theory of radiative transfer in natural media, the coherence matrix for backscatter in a volume layer is expressed as

$$T_v^{ref} = \frac{1}{2}\begin{bmatrix} |1+\gamma|^2 & (\gamma+1)(\gamma-1)^* & 2(\gamma+1)\rho^* \\ (\gamma+1)^*(\gamma-1) & |\gamma-1|^2 & 2(\gamma-1)\rho^* \\ 2(\gamma+1)^*\rho & 2(\gamma-1)^*\rho & 4|\rho|^2 \end{bmatrix}, \quad (18)$$

where γ and ρ are the ratio of HH and HV backscatters to VV backscatter in volume scattering, respectively, and are expressed as follows:

$$\gamma = \frac{\langle (S_{hh} + S_{vv}) S_{hv}^* \rangle + \langle (S_{hh} - S_{vv}) S_{hv}^* \rangle}{\langle (S_{hh} + S_{vv}) S_{hv}^* \rangle - \langle (S_{hh} - S_{vv}) S_{hv}^* \rangle},$$
$$\rho = \frac{2\langle |S_{hv}|^2 \rangle}{\langle (S_{hh} + S_{vv}) S_{hv}^* \rangle - \langle (S_{hh} - S_{vv}) S_{hv}^* \rangle}. \quad (19)$$

In this paper, we suggest that the reference volume scattering coherence matrix can be used to determine the best fit parameters to express the general volume scattering coherence matrix. We first determine the reference coherence matrix T_v^{ref}, as in Eq. (18). Then, we implement finding the volume scattering coherence matrix such that $T_v(\bar{\theta}, \nu)$ approximates to the reference volume scattering coherence matrix by varying randomness ν and mean orientation angle $\bar{\theta}$ for their entire range.[20] These parameter sets are equivalent to the best fit under condition that the Frobenius norm of subtraction of general volume scattering coherence matrix and reference volume scattering coherence matrix becomes a minimum. Therefore, the optimization criteria is

$$\min : \|T_v(\bar{\theta}, \nu) - T_v^{ref}\|_2^2. \quad (20)$$

Finally, we repeat both the aforementioned steps for each pixel in the image. When the generalized volume coherence matrix is determined, we can obtain canopy phase ϕ_v and the coefficient f_v as follows:

$$f_v = \frac{T_{22} - T_{33}}{T_{v(22)} - T_{v(33)}}, \quad \phi_v = \arg\left\{\frac{\Omega_{22} - \Omega_{33}}{T_{v(22)} - T_{v(33)}}\right\}, \tag{21}$$

where Ω_{ij}, T_{ij}, and $T_{v(ij)}$ represent the element of the column j and the row i of the matrix Ω, T, and T_v, respectively.

3.2 *Underlying Ground Topography Phase Estimation*

In order to estimate the ground phase by using the cancellation of scattering mechanism method, we first extract ground and tree-trunk parameters using decomposition techniques. Based on the original Freeman–Durden decomposition, we consider one model for the surface scattering and double-bounce scattering component that have been developed to include full wave depolarization. The coherence matrices for the single-bounce scattering T_g and double-bounce scattering T_d are expressed as follows:

$$T_g = \begin{bmatrix} 1 & \beta\tau & 0 \\ \beta^*\tau & |\beta|^2\kappa & 0 \\ 0 & 0 & |\beta|^2(1-\kappa) \end{bmatrix}, \quad T_d = \begin{bmatrix} |\alpha|^2 & \alpha\tau & 0 \\ \alpha^*\tau & \kappa & 0 \\ 0 & 0 & (1-\kappa) \end{bmatrix}. \tag{22}$$

From Eq. (22), we show that two depolarizing parameters, κ and τ, are added in the original Freeman–Durden decomposition, both of which are related to the distribution function (as yet unknown). These models have the correct boundary conditions: when $\kappa = 1$, $\tau = 1$, two matrices T_g and T_d tend to the single- and double-bounce coherence matrix as proposed by Freeman and Durden (not able to account for the depolarization effect) corresponding to a very smooth surface,[25] whereas when $\kappa = 0.5$, $\tau = 0$, the surface tends to an azimuthally symmetric depolarizer corresponding to a very rough surface.

To accurately extract ground and tree-trunk parameters, the volume scattering component from canopy layer must be removed from the coherence matrices in Eq. (15), whereas the ground and double-bounce scattering components should be retained. When the proper T_v, f_v, and ϕ_v are extracted from adaptive model-based decomposition approach, we obtain new coherence matrices by removing the volume scattering component from the original coherence matrices:

$$\begin{aligned} T^{new} &= T - f_v T_v = f_g T_g + f_d T_d, \\ \Omega^{new} &= \Omega - e^{j\phi_v} f_v T_v = e^{j\phi_g} f_g T_g + e^{j\phi_d} f_d T_d. \end{aligned} \tag{23}$$

From these equations, we can see that there are six unknown parameters $\{f_g, f_d, \beta, \alpha, \kappa, \tau\}$ and four complex observables in matrix T^{new}. This formulation leads to a determined nonlinear equation system. Therefore, to determine the rest of the unknown parameters $\{f_g, f_d, \beta, \alpha, \kappa, \tau\}$ simultaneously, the nonlinear least-squares optimization method is implemented. With each pair of value (κ, τ), the parameter set $\{f_s, f_d, \beta, \alpha\}$ is determined by employing the modified ESPRIT-based PolInSAR.[6] Since the parameter set $\{f_g, f_d, \beta, \alpha, \kappa, \tau\}$ in this step is determined from condition minimum of Frobenius norm of matrix $T^{sub} = T^{new} - (f_g T_g + f_d T_d)$. We show that the parameter set $\{f_g, f_d, \beta, \alpha, \kappa, \tau\}$ is equivalent to the best fit under the condition that the Frobenius norm of the subtraction matrix T^{sub} becomes zero, where the estimated parameters are perfectly matched to the observations.

The ground phase can be estimated by using the cancellation of scattering mechanism method. The complex interferometric coherence for both remainder layers can be derived by using new coherence matrices.

$$\tilde{\gamma}_{\mathrm{gd}} = \tilde{\gamma}_{\mathrm{g}}(\vec{\omega}_1,\vec{\omega}_2) + \tilde{\gamma}_{\mathrm{d}}(\vec{\omega}_1,\vec{\omega}_2) = \frac{\vec{\omega}_1^{*T}\Omega^{\mathrm{new}}\vec{\omega}_2}{\sqrt{(\vec{\omega}_1^{*T}T_1^{\mathrm{new}}\vec{\omega}_1)(\vec{\omega}_2^{*T}T_2^{\mathrm{new}}\vec{\omega}_2)}}$$
$$= \frac{e^{j\phi_{\mathrm{g}}}f_{\mathrm{g}}\vec{\omega}_1^{*T}T_{\mathrm{g}}\vec{\omega}_2}{\sqrt{(f_{\mathrm{g}}\vec{\omega}_1^{*T}T_{\mathrm{g}}\vec{\omega}_1 + f_{\mathrm{d}}\vec{\omega}_1^{*T}T_{\mathrm{d}}\vec{\omega}_1)(f_{\mathrm{g}}\vec{\omega}_2^{*T}T_{\mathrm{g}}\vec{\omega}_2 + f_{\mathrm{d}}\vec{\omega}_2^{*T}T_{\mathrm{d}}\vec{\omega}_2)}}$$
$$+ \frac{e^{j\phi_{\mathrm{d}}}f_{\mathrm{d}}\vec{\omega}_1^{*T}T_{\mathrm{d}}\vec{\omega}_2}{\sqrt{(f_{\mathrm{g}}\vec{\omega}_1^{*T}T_{\mathrm{g}}\vec{\omega}_1 + f_{\mathrm{d}}\vec{\omega}_1^{*T}T_{\mathrm{d}}\vec{\omega}_1)(f_{\mathrm{g}}\vec{\omega}_2^{*T}T_{\mathrm{g}}\vec{\omega}_2 + f_{\mathrm{d}}\vec{\omega}_2^{*T}T_{\mathrm{d}}\vec{\omega}_2)}} \tag{24}$$

with

$$T_1^{\mathrm{new}} = T_1 - f_{\mathrm{v}}T_{\mathrm{v}},$$
$$T_2^{\mathrm{new}} = T_2 - f_{\mathrm{v}}T_{\mathrm{v}}. \tag{25}$$

It is important to note that $\tilde{\gamma}_{\mathrm{g}}(\vec{\omega}_1,\vec{\omega}_2)$ and $\tilde{\gamma}_{\mathrm{d}}(\vec{\omega}_1,\vec{\omega}_2)$ may be considered as coherences only when one of them is zero. In Eq. (24), if a pair of projection vectors $(\vec{\omega}_1,\vec{\omega}_2)$ is properly selected, it may be possible to cancel the ground contribution, in terms of the numerator, in the complex correlation coefficient:[17]

$$(\vec{\omega}_1^{\mathrm{g}})^{*T}T_{\mathrm{g}}\vec{\omega}_2^{\mathrm{g}} = 0. \tag{26}$$

In the same way, the cancellation of the double-bounce contribution may be achieved, with different pairs of projection vectors, as follows:

$$(\vec{\omega}_1^{\mathrm{d}})^{*T}T_{\mathrm{d}}\vec{\omega}_2^{\mathrm{d}} = 0. \tag{27}$$

The proper selection of the projection vector $\vec{\omega}_i^{\mathrm{d}}$ or $\vec{\omega}_i^{\mathrm{g}}(i=1,2)$ may cancel the double-bounce or the ground contributions such that the interferometric phase, neglecting the effect of ϕ_{g}, will either correspond to the ground or the double-bounce contribution. The way to solve this problem is to find the condition under which $\vec{\omega}_i^{\mathrm{d}}$ cancels the double-bounce contribution. The cancellation of double-bounce contribution may be derived by choosing $\vec{\omega}_i^{\mathrm{d}}$ to be an eigenvector of the matrix T_{d}. Based on the optimum parameter set $\{f_{\mathrm{g}}, f_{\mathrm{d}}, \beta, \alpha, \kappa, \tau\}$ that is extracted by using a nonlinear least-squares optimization method, we can choose a pair of projection vectors $(\vec{\omega}_1^{\mathrm{d}},\vec{\omega}_2^{\mathrm{d}})$ for cancellation of the double-bounce contribution. If the single-bounce scattering component is dominant, then the pair of projection vectors $(\vec{\omega}_1^{\mathrm{d}},\vec{\omega}_2^{\mathrm{d}})$ is expressed as

$$\vec{\omega}_1^{\mathrm{d}} = [\,1 \quad a \quad 1\,]^T \quad \vec{\omega}_2^{\mathrm{d}} = [\,1 \quad -a \quad -|a|^2\,]^T \tag{28}$$

with

$$a = \frac{1}{\tau_{\mathrm{opt}}}\frac{e_1(1) + \sqrt{\lambda_r}k^{-1}e_1(2)e^{-j\xi}}{e_2(1) + \sqrt{\lambda_r}k^{-1}e_2(2)e^{-j\xi}} \quad \lambda_r = \frac{\lambda_2}{\lambda_1}, \tag{29}$$

where λ_i denotes the i'th eigenvalue of matrix T^{new}. The coefficients $e_i(j)\ \{i,j=1,2\}$ represent the j'th element of corresponding eigenvector of the i'th eigenvalue of the matrix T^{new}. The coefficients k and ξ are elements of unitary matrix as in Ref. 6. We note that, despite the fact that the double-bounce or the ground contributions may be cancelled, the phase component of the complex coherence will still contain polarimetric as well as interferometric contributions. When the double-bounce contribution is cancelled in terms of the complex correlation coefficient, we can obtain some expressions related to the ground topography phase as follows:

$$(\vec{\omega}_1^{\mathrm{d}})^{*T}\Omega^{\mathrm{new}}\vec{\omega}_2^{\mathrm{d}} = e^{j\phi_{\mathrm{g}}}e^{-\frac{2\sigma h_{\mathrm{v}}}{\cos\theta}}(\vec{\omega}_1^{\mathrm{d}})^{*T}T_{\mathrm{g}}\vec{\omega}_2^{\mathrm{d}}. \tag{30}$$

If the projection vectors are inverted, then

$$(\vec{\omega}_2^{\mathrm{d}})^{*T}\Omega^{\mathrm{new}}\vec{\omega}_1^{\mathrm{d}} = e^{j\phi_{\mathrm{g}}}e^{-\frac{2\sigma h_{\mathrm{v}}}{\cos\theta}}(\vec{\omega}_2^{\mathrm{d}})^{*T}T_{\mathrm{g}}\vec{\omega}_1^{\mathrm{d}}. \tag{31}$$

According to Ref. 18, we can estimate the ground topography phase as follows:

$$\begin{aligned}\arg\{(\vec{\omega}_1^{\,\mathrm{d}})^{*T}\Omega^{\mathrm{new}}\vec{\omega}_2^{\,\mathrm{d}}\} &= \phi_{\mathrm{g}} + \arg\{(\vec{\omega}_1^{\,\mathrm{d}})^{*T}T_{\mathrm{g}}\vec{\omega}_2^{\,\mathrm{d}}\}\\ \arg\{(\vec{\omega}_2^{\,\mathrm{d}})^{*T}\Omega^{\mathrm{new}}\vec{\omega}_1^{\,\mathrm{d}}\} &= \phi_{\mathrm{g}} - \arg\{(\vec{\omega}_2^{\,\mathrm{d}})^{*T}T_{\mathrm{g}}\vec{\omega}_1^{\,\mathrm{d}}\},\end{aligned} \tag{32}$$

$$\phi_{\mathrm{g}} = \frac{1}{2}\{\arg\{(\vec{\omega}_1^{\,\mathrm{d}})^{*T}\Omega^{\mathrm{new}}\vec{\omega}_2^{\,\mathrm{d}}\} + \arg\{(\vec{\omega}_2^{\,\mathrm{d}})^{*T}\Omega^{\mathrm{new}}\vec{\omega}_1^{\,\mathrm{d}}\}\}. \tag{33}$$

3.3 *Forest Height Estimation*

One of the simplest approaches to height estimation is to use the phase difference between interferogram as a direct estimate of height. The forest height first can be extracted by using the phase differencing between the canopy phase and ground phase, as in Eq. (34):[25]

$$h_{\mathrm{v}} = \frac{\phi_{\mathrm{v}} - \phi_{\mathrm{g}}}{k_z} = \Delta\phi\frac{\lambda}{4\pi}\frac{R\,\sin\,\theta}{B\,\cos(\theta-\delta)}, \tag{34}$$

where θ is the mean angle of incidence, R is the distance between radar and an observed point, δ is the baseline tilt angle, B is the baseline, and λ is the wavelength.

In order to improve the accuracy of forest height estimation, we first use forest height, which is estimated by GTLSM, exactly as proposed in Eq. (34). In Ref. 26, Chen demonstrated that the interferometry phase corresponding to canopy increases with real forest height. The difference between the actual forest and canopy height is called the penetrated depth. The penetrated depth depends on the incident angle, forest species, and forest shape. We show that the penetrated depth does not change with real forest height. Hence, the scattering center of canopy is always lower than the forest height. This is why we cannot use the canopy scattering center to represent the top of the canopy. Hence, the true forest height is always underestimated. To progress, one key idea is that this error can be at least partly compensated by employing a coherence amplitude correction term, as introduced by Cloude.[25] Finally, by combining these two terms with a scaling parameter η, we then obtain an approximate algorithm that can compensate for the variation in structure, as shown in Eq. (35):[25]

$$h_{\mathrm{v}} = \Delta\phi\frac{\lambda}{4\pi}\frac{R\,\sin\,\theta}{B\,\cos(\theta-\delta)} + \eta\frac{\pi - 2\,\arcsin(|\tilde{\gamma}_{\mathrm{v}}|^{0.8})}{k_z}, \tag{35}$$

where $\tilde{\gamma}_{\mathrm{v}}$ denotes the complex coherence for the volume alone. In Eq. (35), the first term represents the phase coherence, whereas the second term is the coherence amplitude correction. This expression has the right kind of behavior in two important special cases. If the medium has a uniform structure function, then the first term will give half the height but the second will then also obtain half the true height (if we set $\eta = 0.5$). At the other extreme, if the structure function in the volume channel is localized near top of the layer, then the phase height will give the true height, and second term will approach zero, which infers the weight set as $\eta = 0$. To reduce the error from change of extinction coefficient and the vertical structure, we select $\eta = 0.4$, as reported in Ref. 25.

Theoretically, the forest height estimation using the GTLSM proposed model from L-band PolInSAR data ranges from 0 to $2\pi/k_z$. However, in practice, the accuracy of forest height estimation depends strongly on some parameters, such as tree density, species, age-related variation, wavenumber, and the wave extinction in the volume scattering layer. When the extinction decreases, waves interact with a thicker layer of the volume, resulting in a more important volume decorrelation due to an increasing scatterer height diversity, and in a diminution of the phase center height in the volume, until half of its height. Therefore, for the GTLSM model, if the forest height is not large enough, the canopy layer will be extended from the crown to the ground. Then, the phase of bottom of all the layers overlaps at the ground (such as in a two-layer RVoG scenario), which is unreliable for the use of the GTLSM model for an estimation of the forest height. Therefore, the minimum forest height estimation using the GTLSM model

approximates half of the forest height estimated from the amplitude coherence. Only a forest higher than 10 m has been investigated to avoid the dominant ground contribution and to ensure no overlap of the bottom phase of the three layers. Due to the limitation of the three-component model, there are problems of negative powers in the proposed method. If $T_{11} < 2T_{33}$, $T_{22} < T_{33}$ or $(T_{11} - 2T_{33})(T_{22} - T_{33}) < |T_{12}|^2$, the powers of single-bounce f_g or double-bounce f_d are negative, and the volume scattering power is overestimated. In order to solve this problem, the preprocessing for PolInSAR data is implemented. The data preprocessing does not change in terms of which scattering component is dominant, and it helps to reduce the overestimation of the volume scattering power. The data preprocessing is represented in Eq. (36):

$$\begin{cases} T_{33} = \min\left(\frac{T_{11}}{2}, T_{22}\right) & \text{if } T_{11} < 2T_{33} \text{ or } T_{22} \\ T_{12} = T_{12}\frac{\sqrt{(T_{11}-2T_{33})(T_{22}-T_{33})}}{|T_{12}|} & \text{if } (T_{11} - 2T_{33})(T_{22} - T_{33}) < |T_{12}|^2 \end{cases}. \tag{36}$$

4 Experimental Results and Discussion

In this section, the effective evaluation of the proposed approach is addressed but primarily in terms of the retrieved forest height estimation and ground phase. For such a purpose, we have applied the GTLSM to a data set acquired from PolSARProSim software by Williams,[27] as well as spaceborne data acquired by SIR-C/X-SAR system from National Aeronautics and Space Administration (NASA).

4.1 *Simulated PolInSAR Data*

The proposed GTLSM model has been evaluated by the simulated forest scenario and by considering different incidence angles, which are generated with the PolSARProSim software. This scenario consists of a distribution of idealized tree corresponding to the forest model as shown in Fig. 1, with a layer of vertical tree trunk extending from 0 to h_d, a canopy layer with depth $r_h h_v$, and forest height h_v. The simulated data are realized at 1.3 GHz with 30-deg angle of incidence, assuming a strong volume scattering component from the canopy, a strong double bounce component from tree trunk, and a medium strength surface scattering component. The interferometer is operated at 10 m horizontal and 1 m vertical baseline. The stand height 18 m is located on a 1% ground azimuth and 2% ground range slope. The forest stand occupies a 0.72854 Ha area, with a stand density is 1000 stem/Ha. The azimuth and slant range resolution are 1.0 and 1.5 m, respectively.

Figure 3 shows a red, green, blue (RGB) coding Pauli image of the forest scenario considered with 143 pixels in range and 131 pixels in azimuth, and the red line indicates the transect analyzed in this paper. The top of image corresponds to far range, which can be identified due to the

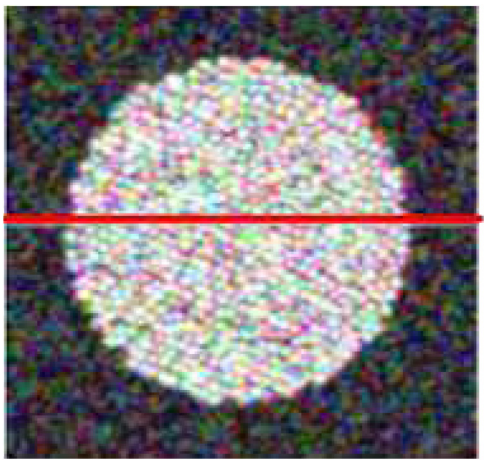

Fig. 3 Pauli image on RGB coding of the simulated data.

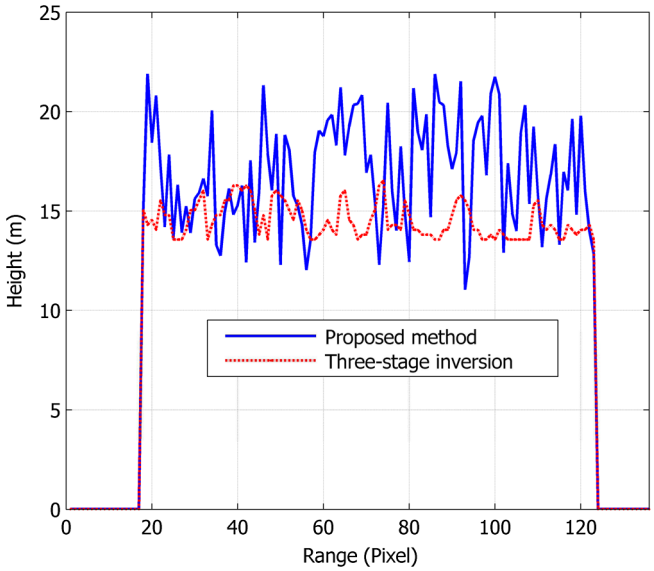

Fig. 4 Profile of the estimated forest heights of selected rows for two approaches.

Table 1 Forest height estimation for two approaches.

Parameter estimation	True	Three-stage inversion + RVoG	Proposed method + GTLSM
h_v (m)	18	14.9881	17.6545
h_d (m)	11	—	10.8279
r_h	2/3	0.4724	0.4500
σ (dB/m)	0.2	0.3168	0.2087
ϕ_g (rad)	0.0148	0.0442	0.0279
RMSE (m)	0	1.5107	2.0779

Note: RVoG, random volume over ground; RMSE, root mean squared error; GTLSM, general three-layer scattering model.

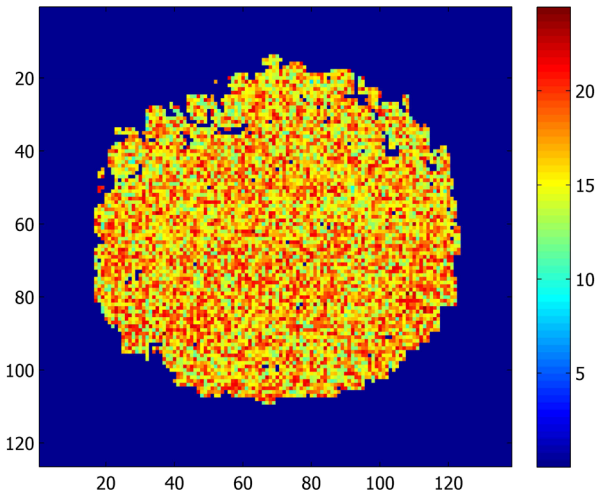

Fig. 5 Forest height is estimated by general three-layer scattering model algorithm.

Table 2 Parameter estimation for two different scenes using GTLSM.

Parameter estimation	$\theta = 45$ deg	$\theta = 60$ deg
h_v (m)	18.4646	19.0592
h_d (m)	12.4273	14.6061
r_h	0.4264	0.4176
ϕ_g (dB/m)	0.0263	0.0286
RMSE (m)	2. 3688	2.4892
P_v/P_{total}	0.5822	0.7855

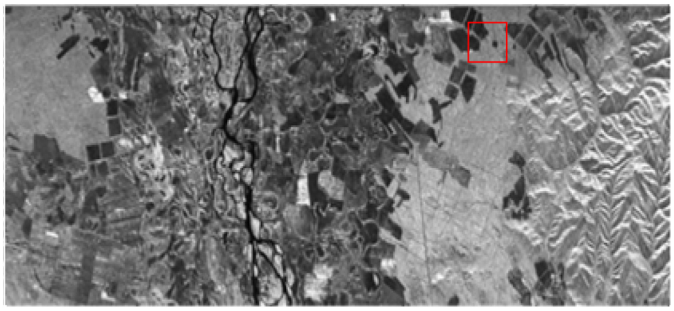

Fig. 6 The total power image of the test area. The red square region shows the selected area for evaluation as forest.

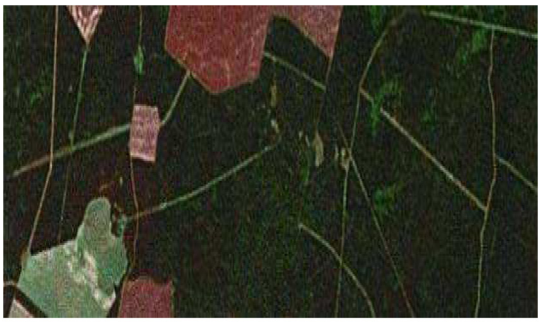

(a)

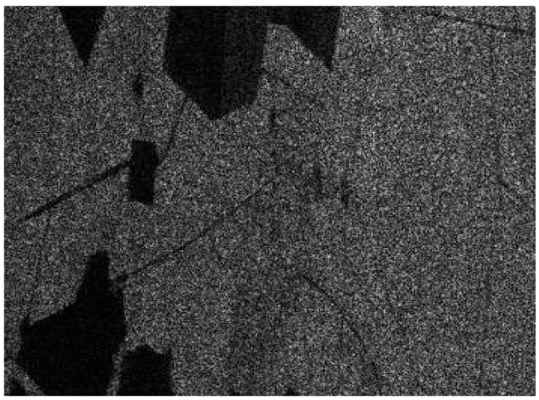

(b)

Fig. 7 Test site in Tien-Shan: (a) optical image and (b) HV amplitude image.

shadowing effect at the borders of the forest. Figure 4 is a plot of the forest height estimation of the proposed approach compared with the three-stage inversion process in the azimuth transects line.[3]

Table 1 indicates that the proposed method is more accurate and has less error than the three-stage inversion process. The three-stage inversion process uses the RVoG model to retrieve forest heights. According to the algorithm, the inversion of forest heights can be divided into three separate stages. The ground phases are extracted in the first two stages by using the line fit method. The forest heights are estimated in the last stage. In these stages, we usually assume that there is not any ground scattering component in the HV channel, and let volume decorrelation be $\tilde{\gamma}_{\mathrm{est,v}} \approx \tilde{\gamma}_{\mathrm{HV}} \exp(-j\phi_{\mathrm{g}})$. We can construct a look-up table (LUT) of volume coherence $\tilde{\gamma}_{\mathrm{v}}$ as a function of forest height h_{v} and the extinction coefficient σ. By comparing $\tilde{\gamma}_{\mathrm{est,v}}$ with the LUT, we can then obtain an estimation of forest heights.

Otherwise, the forest height and extinction estimation by using three-stage inversion process becomes inappropriate for dense forest region due to strong attenuation of electromagnetic in the ground medium, and only the underlying ground topographic phase is reliable. Based on Fig. 4

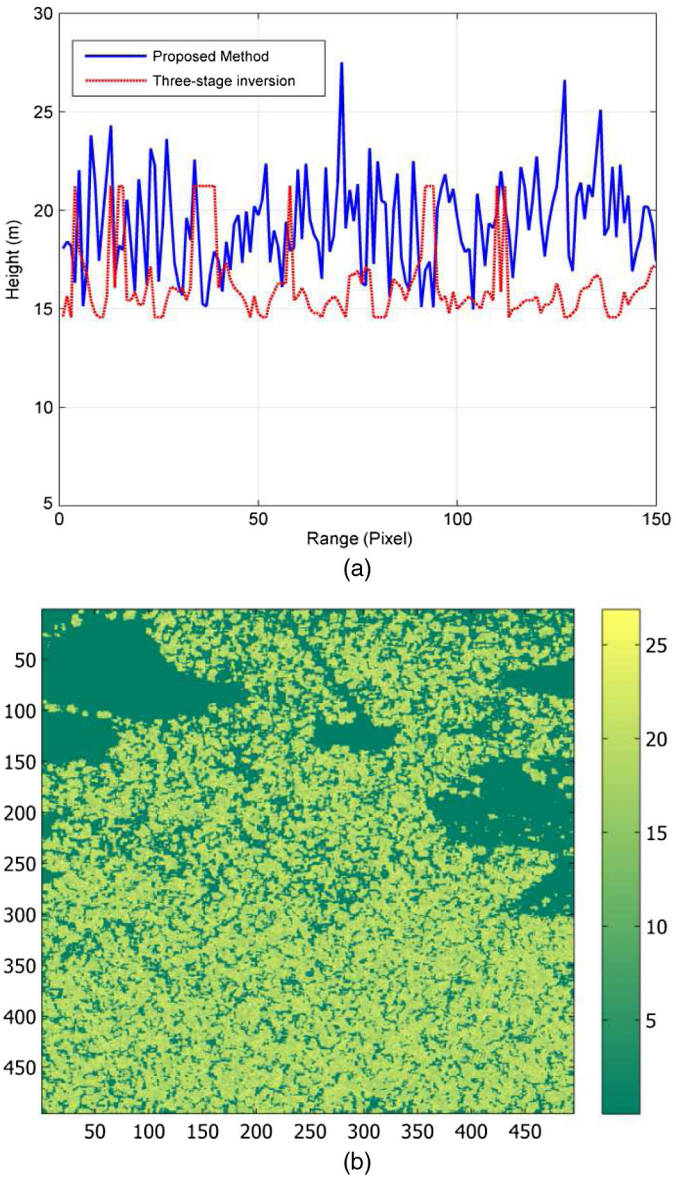

Fig. 8 Forest height estimation. (a) Profile of the estimated forest heights of selected rows for two approaches and (b) forest height estimation from proposed algorithm.

Table 3 Forest parameters estimation from two approaches.

Parameter estimation	Three-stage inversion + RVoG	Proposed method + GTLSM
h_v (m)	17.7898	20.1146
h_d (m)	–	15.2033
r_h	0.4572	0.4764
σ (dB/m)	0.2143	0.1553
ϕ_g (rad)	–0.0606	–0.0535
RMSE (m)	3.3880	3.5729

and Table 1, we can say that the forest height and ground phase estimation by using the GTLSM is more accurate and reliable than its by using three-stage inversion process.

The forest height estimation by using the GTLSM is shown in Fig. 5. In this figure, it is shown that the peak differential of the forest height is located at ∼18 m. The actual forest heights are quite well-retrieved, except that some pixels are overestimated but most forest heights in these pixels are all less than 22 m. The real effective forest height will be higher than these values; we can say that these results are acceptable. Likewise, the proposed method provides relative accuracy with small error and is more accurate for vertical structure variations.

Changes in the scene parameters can be noticed by means of the proposed approach. Table 2 shows the estimation of forest parameters when incidence angle is 45 and 60 deg. The rest of parameters remain unchanged. When steeper incidence angles are used, since the attenuation of electromagnetic through the canopy layer becomes stronger, and the direct ground backscatter that grows into it is also noticeable. Therefore, the forest height and ground phase become overestimated, whereas the fraction fill canopy of the tree is underestimated when the incidence angle increases. From Table 2, we show that as the incidence angle increases, the power of the volume contribution also increases. In these scenes, the volume component is dominant.

4.2 *Spaceborne PolInSAR Data*

Next, we have also tested the performance of the proposed GTLSM with spaceborne data. In the present study, the data used consists of two SIR-C single look complex image pair of the

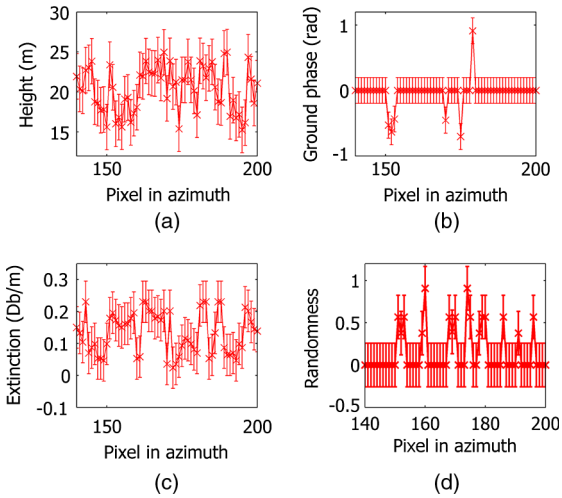

Fig. 9 Parameter estimation for test site area. (a) Forest height estimation, (b) ground phase estimation, (c) the mean volume extinction coefficient, and (d) the degree of orientation randomness of volume scattering contribution.

Tien-Shan test site by the SIR-C/X-SAR system on October 7 and 9, 1994 (data takes 122.20 and 154.20). They consist of quad-pol interferometric data at L-band with a 24.569 deg angle of incidence and 60 m baseline. The total power image of the test area is shown in Fig. 6.

After coregistration of PolInSAR images, we select evaluation area with 495 pixels in range and 495 pixels in azimuth. The evaluation region has a mixed forestry, road, and agricultural area. Figure 7(a) is the optical image of the evaluation patch and Fig. 7(b) is the HV amplitude image of test area for evaluation as forest. The Tien-shan area contains heterogeneous objects such as forest area (green area), agriculture, and road (red area).

Figure 8(a) is a plot of forest height estimation of the proposed approach compared with three-stage inversion process of a selected row, i.e., 150th to 250th. The parameters of forest by using two methods are calculated and shown in Table 3. This table indicates that the forest parameters' estimation by using the GTLSM are more accurate and less error-prone than by using the three-stage inversion. Figure 8(b) shows the estimated forest height by the proposed approach in the test site. This figure shows that most of the peak differential of the forest height is located at ∼20 m. The forest height estimation at some pixels is overestimated by less than 30 m. However, these values are almost lower than the 2π height ambiguities, which are about 32 m; so, we can say that the results are acceptable. Based on Fig. 8 and Table 3, we can say the height forest estimation and the underlying ground topographic phase are reliable. Consequently, the proposed approach provides relative accuracy with a small error and is more accurate for vertical structure variations.

To estimate the main forest parameters, the optimization algorithm is used. The parameter inversion process consists in optimizing the error function and estimating the physical parameters $\{h_v, h_d, r_h, f_v, \bar{\theta}, \nu, f_d, \alpha, f_g, \beta, \kappa, \tau\}$. Figure 9 presents the parameter inversion performance in the 200th row of the test site. The height sensitivity is given by the vertical wavenumber which is about 0.2. This corresponds to 2π height ambiguity of about 32 m. In the experiments, the graphs display the value and the standard deviation of estimated parameters. This figure indicates that the total forest height is around 20 m [Fig. 9(a)], the underlying topographic phase is varied in ranges from −0.5 to 0.5 rad [Fig. 9(b)], the mean volume extinction coefficient is around 0.16 dB/m [Fig. 9(c)], and the degree of orientation randomness of volume scattering contribution is very low ($\nu \approx 0$) [Fig. 9(d)].

5 Conclusions

The GTLSM has been developed that allows flexible modeling of natural forest for which existing two-layer or three-layer RVoG models are inappropriate. The proposed GTLSM separated the vertical structure of forest into three layers corresponding to the canopy layer, tree-trunk layer, and ground layer that allow us to consider the simultaneous effect of three types scattering mechanisms in the forest region. In the GTLSM, the canopy parameters are extracted by using adaptive model-based decomposition technique based on an interferometric coherence matrix, whereas underlying ground topography phase is estimated by the cancellation mechanism based on the correlation coefficient. In comparison to three-stage inversion method, the proposed approach enables us to improve the accuracy of forest height and ground topography estimations, as well as to retrieve additional parameters related to the degree of randomness, the main orientation of particles, and the depth of the canopy layer and power contribution of each scattering component. The GTLSM is quite flexible and effective for analysis of a more complex multilayer forest model with PolInSAR images. Experimental results indicate that the forest parameters can be retrieved directly and more accurately by the proposed GTLSM.

References

1. FAO, "Global forest resources assessment 2005," *FAO Forestry Paper*, p. 147 (2005).
2. C. L. Martinez, X. Fabregas, and L. Pipia, "Forest parameter estimation in the PolInSAR context employing the multiplicative-additive speckle noise model," *J. Photogramm. Remote Sens.* **66**, 597–607 (2011).

3. S. R. Cloude and K. P. Papathanassiou, "Three-stage inversion process for polarimetric SAR interferometric," *IEEE Proc. Radar Sonar Navig.* **150**(3), 125–134 (2003).
4. H. Yamada et al., "Polarimetric SAR interferometry for forest analysis based on the ESPRIT algorithm," *IEICE Trans. Electron.* **E84-C**(12), 1917–2014 (2001).
5. H. Yamada et al., "Polarimetric SAR interferometric for forest canopy analysis by using the super-resolution method," in *Proc. of IEEE Int. Geoscience and Remote Sensing Symp.*, pp. 1101–1103, Sydney, Australia (2001).
6. H. Yamada, M. Yamazaki, and Y. Yamaguchi, "On scattering model decomposition of PolSAR and its application to ESPRIT-based PolInSAR," in *Proc. of 6th European Conf. on Synthetic Aperture Radar* (2006).
7. F. Garestier and T. Le Toan, "Evaluation of forest modeling for forest height estimation using P-band PolInSAR data," in *Proc. BIOGEOSAR*, Bari, Italy (2007).
8. F. Garestier and T. Le Toan, "Forest modeling for forest height inversion using single baseline InSAR/PolInSAR data," *IEEE Trans. Geosci. Remote Sens.* **48**(3), 1528–1539 (2010).
9. F. Garestier and T. Le Toan, "Estimation of the backscatter vertical profile of a pine forest using single baseline P-band (Pol-) InSAR data," *IEEE Trans. Geosci. Remote Sens.* **48**(9), 3340–3348 (2010).
10. J. D. Ballester-Bermand and J. M. Lopez-Sanchez, "Applying the Freeman-Durden decomposition concept to polarimetric SAR interferometry," *IEEE Trans. Geosci. Remote Sens.* **48**(1), 466–479 (2010).
11. J. D. Ballester-Bermand and J. M. Lopez-Sanchez, "Combination of direct and double-bounce ground responses in the homogeneous oriented volume over ground model," *IEEE Geosci. Remote Sens. Lett.* **8**(1), 54–58 (2011).
12. R. N. Treuhaft and P. Siqueria, "Vertical structure of vegetated land surface from interferometric and polarimetric Radar," *Radio Sci.* **35**(1), 141–177 (2000).
13. S. R. Cloude and K. P. Papathanassiou, "Polarimetric SAR interferometry," *IEEE Trans. Geosci. Remote Sens.* **36**(5), 1551–1565 (1998).
14. A. Porte et al., "Allometric relationships for branch and tree woody biomass of maritime pine (Pinus Pinaster Ait)," *For. Ecol. Manage.* **158**(1), 71–83 (2002).
15. N. P. Minh, B. Zou, and C. Yan, "Forest height estimation from PolInSAR image using adaptive decomposition method," in *Proc. of 11th Int. Conf. Image Processing*, pp. 1830–1834, Beijing, China (2012).
16. P. E. Gill and W. Murray, "Algorithms for the solution of the nonlinear least-square problems," *SIAM J. Numer. Anal.* **15**(5), 977–992 (1978).
17. C. L. Martinez and K. P. Papathanassiou, "Cancellation of scattering mechanism in PolInSAR: application to underlying topography estimation," *IEEE Trans. Geosci. Remote Sens.* **51**(2), 953–965 (2013).
18. C. Lopez-Martinez et al., "Ground topography estimation over forests considering polarimetric SAR interferometry," in *Proc. IEEE Int, Geoscience and Remote Sensing Symp.*, pp. 3612–3615 (2010).
19. A. Freeman and S. L. Durden, "A three component scattering model to describe polarimetric SAR data," *IEEE Trans. Geosci. Remote Sens.* **36**(3), 963–973 (1998).
20. M. Arri, J. VanZyl, and Y. Kim, "Adaptive model-based decomposition of polarimetric SAR covariance matrix," *IEEE Trans. Geosci. Remote Sens.* **49**(3), 1104–1113 (2011).
21. M. Arri, J. VanZyl, and Y. Kim, "A general characterization for polarimetric scattering from vegetation canopies," *IEEE Trans. Geosci. Remote Sens.* **48**(9), 3349–3357 (2010).
22. S. R. Cloude and E. Pottier, "An entropy based classification scheme for land application of polarimetric SAR," *IEEE Trans. Geosci. Remote Sens.* **35**(1), 68–78 (1997).
23. S. R. Cloude and E. Pottier, "A review of target decomposition theorems in radar polarimetry," *IEEE Trans. Geosci. Remote Sens.* **34**(2), 498–518 (1996).
24. A. Karma et al., "A microwave polarimetric scattering model for forest canopies based on vector radiative transfer theory," *Remote Sens. Environ.* **53**(1), 16–30 (1995).
25. S. R. Cloude, "Polarization application in remote sensing," Oxford University Press, pp. 284–339, New York (2009).
26. C. J. Hong, Z. Hong, and W. Chao, "Comparison between ESPRIT algorithm and three-stage algorithm for PolInSAR," in *Proc. of Int. Conf. on Multimedia Technology*, pp. 1–3 (2010).

27. M. L. Williams, "PolSARproSim: A coherent, polarimetric SAR simulation of Forest for PolSARPro," http//earth.eo.esa.int/polsarpro/SimulatedDataSources.html (December 2006).

Nghia Pham Minh received his BS and MS degrees in electronics engineering from the Le Qui Don Technical University, Hanoi, Vietnam, in 2005 and 2008, respectively, and his PhD degree in information and communication engineering from the Harbin Institute of Technology (HIT), China, in 2014. He is currently a lecturer with the faculty of Radio-Electronics, Le Qui Don Technical University, Hanoi, Vietnam. He currently focuses on polarimetric synthetic aperture radar (PolSAR) image processing, polarimetric SAR interferometry, and signal processing.

Bin Zou received his BS degree from the HIT, Harbin, China, in 1990, his MS degree in space studies from the International Space University, Strasbourg, France, in 1998, and his PhD degree in 2001. He is currently a professor and vice head of the Department of Information Engineering, School of Electronics and Information Technology, HIT. He currently focuses on synthetic aperture radar (SAR) image processing, PolSAR, PolSAR interferometry, hyperspectral imaging, and data processing.

Yan Zhang received her BS and MS degrees from the HIT, Harbin, China, in 2012 and 2014, respectively. She is currently working at 360 Company, Beijing, China. Her research interests are mainly high-frequency electromagnetic computing, PolSAR interferometry, hyperspectral imaging, and data processing.

Vannhu Le received his BS degree from Le Quy Don Technical University, Hanoi, Vietnam, in 2007 and his MS degree from the HIT in 2012. Now, he is pursuing his PhD degree at the Research Center for Space Optics Engineering, HIT, Harbin, China. He currently focuses on image processing, optical image processing, and optical system design.